Journal of Luminescence 130 (2010) 2476–2486

Contents lists available at ScienceDirect

Journal of Luminescence

journal homepage: www.elsevier.com/locate/jlumin

Spectroscopic and nano-molecular modeling investigation on the binary and ternary bindings of colchicine and lomefloxacin to Human serum albumin with the viewpoint of multi-drug therapy

J. Chamani [a,*], A. Asoodeh [b], M. Homayoni-Tabrizi [a], Z. Amiri Tehranizadeh [c], A. Baratian [c], M.R. Saberi [c], M. Gharanfoli [d]

[a] Department of Biology, Faculty of Sciences, Islamic Azad University-Mashhad Branch, Mashhad, Iran
[b] Department of Chemistry, Faculty of Sciences, Ferdowsi University of Mashhad, Mashhad, Iran
[c] Medical Chemistry Department, School of Pharmacy, Mashhad University of Medical Sciences, Mashhad, Iran
[d] Department of Development Biology, Culture and Science University, Tehran, Iran

ARTICLE INFO

Article history:
Received 21 April 2010
Received in revised form
14 August 2010
Accepted 18 August 2010
Available online 26 August 2010

Keywords:
HSA
Lomefloxacin
Colchicine
Spectroscopy
Molecular dynamic

ABSTRACT

Combination of several drugs is often necessary especially during long-term therapy. The competitive binding drugs can cause a decrease in the amount of drug bound to protein and increase the biological active fraction of the drug. The aim of this study is to analyze the interactions of Lomefloxacin (LMF) and Colchicine (COL) with human serum albumin (HSA) and to evaluate the mechanism of simultaneous binding of LMF and COL to protein. Fluorescence analysis was used to estimate the effect of drugs on the protein fluorescence and to define the binding and quenching properties of drugs-HSA complexes. The binding sites for LMF and COL were identified in tertiary structure of HSA with the use of spectrofluorescence analysis. The analysis of fluorescence quenching of HSA in the binary and ternary systems show that LMF does not affect the complex formed between COL and HSA. On the contrary, COL decreases the interaction between LMF and HSA. The results of synchronous fluorescence, resonance light scattering and circular dichroism spectra of binary and ternary systems show that binding of LMF and COL to HSA can induce micro-environmental and conformational changes in HSA. The simultaneous presence of LMF and COL in binding to HSA should be taken into account in the multi-drug therapy, and necessity of using a monitoring therapy owning to the possible increase of the uncontrolled toxic effects. Molecular modeling of the possible binding sites of LMF and COL in binary and ternary systems to HSA confirms the spectroscopic results.

1. Introduction

Human serum albumin (HSA) is the most abundant carrier protein in blood circulation that can bind many endogenous and exogenous compounds e.g. fatty acids, bilirubin, prostaglandins, steroids, cholesterol, uric acid, hormones, drugs and contrasting substances reversibly, with dissociation binding constant (K_D) in the range of 10^{-3}–10^{-8} mol L^{-1} [1]. The structure of HSA has been determined crystallographically [2,3] and discovered that it consisted of three structurally homologous, predominantly helical domains (domain I, II and III), which each domain contained two sub-domains (A and B). Two principal binding sites were located in sub-domains IIA and IIIA, which are named as site I and site II, respectively. The drugs bound in site I are generally bulky heterocyclic anions with the charge situated in a central position of the molecules and that in site II are aromatic carboxylic acids with an extended conformation and the negative charge located at one end of the molecule [4,5]. HSA is a globular protein composed of a single polypeptide chain of 585 amino acid residues with a largely alpha-helical structure. Its amino acid sequence contains a total of 17 disulfide bridges, one free thiol (Cys-34) and a single tryptophan (Trp-214). It is capable of binding a wide variety of drugs and xenobiotics [6–11]. Binding of drugs to plasma proteins is an important pharmacological parameter, since it frequently affects the distribution and elimination of a drug as well as the duration and intensity of its physiological action [12–14]. Drugs, which are administered in multi-drug therapy, may alter each others binding to the transporting protein. Therefore, it is necessary to determine both the location of the binding sites and the possible interactions for each individual drug. Combination of several drugs is often required, especially during long-term therapy. The simultaneous presence of two drugs for the binding sites on HSA may result in decrease in binding and hence increase in the concentration of free biologically active fraction of one or both the drugs. HSA is a flexible molecule and binding of a drug often affects the simultaneous binding of other

* Corresponding author. Tel.: +98511 8437107; fax: +98511 8424020.
E-mail address: Chamani@ibb.ut.ac.ir (J. Chamani).

0022-2313/$ - see front matter © 2010 Elsevier B.V. All rights reserved.
doi:10.1016/j.jlumin.2010.08.016

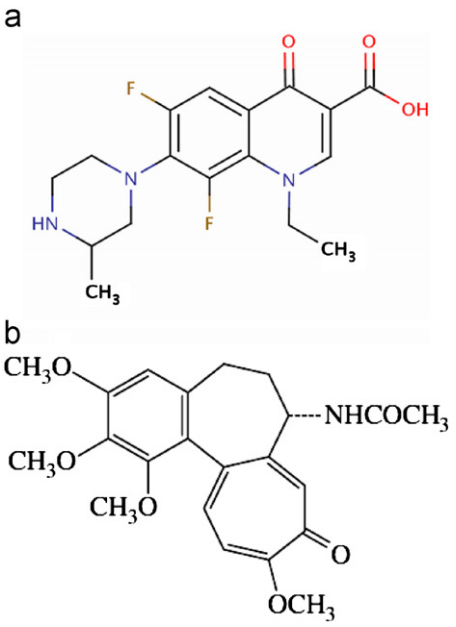

Fig. 1. (a) Structure of lomefloxacin and (b) structure of colchicine.

drugs. Therefore, study of the interaction between HSA and drugs is imperative and can obtain a lot of information of drug actions.

Lomefloxacin (LMF, Fig. 1a) is an antibiotic in a class of drugs called fluoroquinolones with a wide spectrum of activity against various bacterial infections, such as bronchitis and urinary tract infections [15]. Colchicine (COL, Fig. 1b) is used for the treatment of acute or chronic gout [16,17]. Colchicine produces its anti-inflammatory effects by binding to the intracellular protein tubulin, thereby preventing its polymerization into microtubulin and leading to the inhibition of leukocyte migration and phagocytosis [18]. This study is designed to analyze the simultaneous interactions of LMF and COL to HSA under physiological conditions. Besides using fluorescence spectroscopic, resonance light scattering, circular dichroism (CD) methods and molecular modeling are also applied. The effects of drugs on the HSA are estimated and the binding constant, the number of binding sites and protein conformational changes of drug-HSA complexes are determined.

2. Materials and methods

2.1. Materials

Human serum albumin (fatty acid free, 90%), lomefloxacin and colchicine were purchased from Sigma Chemical Co. (St. Louis, MO, USA). All reagents were used as supplied without further purification. The protein was dissolved in 50 mM phosphate buffer solutions at pH 7.4 and the stock solution was kept in the dark at 4 °C. All other reagents were of analytical grade and doubly distilled water used through out all the experiments.

2.2. Fluorescence measurements

Fluorescence spectra were recorded at room temperature with a Eclips carry fluorimeter (Varian, USA) using 5 nm × 5 nm slit widths, equipped with a thermostatically controlled cell holder in the range of 315–500 nm (at an excitation wavelength of 295 nm) and 300–500 nm (at an excitation of 280 nm) individually, and the emission spectra of the free HSA and HSA-drug mixtures were measured using the buffer solutions of drugs in corresponding concentration as reference. Measurements were performed for each studied drug using HSA solution, (1) with a single drug (LMF or COL) of various concentrations and (2) with the two drugs, which were added simultaneously to HSA.

A dilution series of drugs were prepared in a 50 mM phosphate buffer. For each data point, 5 μl of the drug solution was added into 2 ml HSA solution. The reaction time has been investigated and the results showed that 3 min was enough for the stabilization. So the change in fluorescence emission intensity was measured within 3 min of adding drugs to the HSA and the concentration of oxygen at the experimental conditions is maintained as a constant. The addition of a constant volume of quencher to the protein solution avoided complications due to dilution effects within titration type experiments. Each measurement was repeated in triplicate and the mean and standard deviation were calculated. The fluorescence quenching data were plotted as relative fluorescence intensity against drug concentrations.

The synchronous fluorescence spectra were obtained by scanning simultaneously the excitation and emission monochromators. The synchronous fluorescence spectra only show the tyrosine and tryptophan residues of HSA when the wavelength interval ($\Delta\lambda$) is 15 nm and 60 nm, respectively [19]. By scanning both the excitation and emission monochromators of a common spectrofluorometer with $\Delta\lambda=0$ nm, a resonance light scattering spectrum can be developed [20], which has been proved to be able to investigate the aggregation of small molecules and the long-range assembly of organic dyes on biological templates [20,21]. All RLS spectra were obtained by scanning simultaneously the excitation and emission monochromators (namely $\Delta\lambda=0$) from 250 to 700 nm with slit widths at 5 nm for the excitation and the emission.

2.3. Circular dichroism measurements

Circular dichroism (CD) measurements were carried out on a Jasco-815 automatic recording spectropolarimeter (Japan) in cell of path length 2 mm at room temperature. The induced ellipticity was obtained by the ellipticity of the drug-HSA mixture subtracting the ellipticity of drug at the same wavelength and is expressed in degrees. The results are expressed as mean residue ellipticity (MRE) in deg. cm^2/dmol, which is defined as [MRE θ_{obs} (mdeg)/10 nlC_p]. The θ_{obs} represents the CD in milli-degree, n is the number of amino acid residues (585), l and C_p are the path length of the cell and the mole fraction, respectively. The alpha-helical content of HSA was calculated from the MRE value at 208 nm using the equation $\alpha\%$ helix=[MRE 208−4000)/33000−4000] × 100 as described by Khan et al. [22].

2.4. Molecular modeling calculations

The crystal structure for human serum albumin (HSA) (PDB ID: 1BM0) was employed in the docking calculation performed with autodock4 on an Ubuntu Linux platform, which combines a rapid energy evaluation through pre-calculated grids of affinity potentials with a variety of search algorithm to find suitable for a ligand on a given macromolecule. The complexes (Colchicine, Lomefloxacin) used in docking calculations were submitted to a pre-minimization with the MM+ force field. All compounds were energy minimized by means of AM1 semi-empirical force field. The energy minimized ligands were further processed using Autodock tools program, adding partial atomic charges for each atom, and defining the rigid root and rotatable bond for each ligand automatically. A grid map for the whole protein structure was generated with the default 0.375 Å spacing by the auto-grid

program. The sigmoidal distance-dependent the electric permittivity of Mehler and Solmajer was used for the calculation of the electrostatic grid maps. The lamarkian genetic algorithm method was applied for minimization, using default parameters and random starting positions on the entire protein area, random orientations and torsions were used for ligands. After determining high affinity area of the protein to the ligands, grid map was restricted to the said area and its amino acids were marked as flexible with default torsions. (LEU115, MET123, TYR161, ILE142, PHE157, LEU182, ARG186 for colchicine; LEU115, MET123, TYR161, ILE142, PHE157, LEU182, ARG186, TYR138 for lomefloxacin; MET123, TYR161, ILE142, PHE157, LEU182, ARG186, TYR138 for lomefloxacin and colchicine; TYR138, ILE142, PHE157, LEU185, ARG117, PHE149, TYR161 for colchicine and lomefloxacin) Number of GA runs was set to 200 for each set; other parameters were left at their defaults [23–25].

3. Results and discussion

3.1. Fluorescence quenching of HSA induced by LMF and COL

Protein fluorescence is quenched by a ligand when the distance between the ligand and the fluorophore in protein is smaller than 10 nm [26]. There is one tryptophan residue in HSA, Trp-214, which is situated in sub-domain IIA [2]. When the excitation wavelength is 295 nm, only the tryptophan residue has a fluorescence emission at about 350 nm and the other one at about 450 nm. The emission wavelengths of 350 and 450 nm are related to HSA and LMF, respectively. With increase in the LMF to the HSA solution, the emission peak at 450 nm increase that enhance the LMF concentration in solution. At the excitation wavelength of 280 nm, both tryptophan and tyrosyl amino acid residues have fluorescence emission. Comparison of fluorescence quenching of protein excited at 280 nm and 295 nm allows estimating the participation of tryptophan and tyrosine groups in the complex. The quenching take place when the ligand (quencher) is sufficiently close to the tryptophanyl or/and tyrosyl residues. Then the energy transfer between a ligand and fluorophore is possible. Fig. 2 shows the fluorescence quenching spectra of HSA excited at 280 and 295 nm in the presence of LMF and COL. LMF and COL have no fluorescence emission at the range measured and the background can be subtracted by using the corresponding concentration of the drugs solutions as reference when recording the spectra. It can be seen from Fig. 2 that the intensities of fluorescence emission of HSA decreased gradually with the increase in drugs concentrations. The quenching curves of HSA excited at 280 and 295 nm in the presence of LMF (Fig. 3a) overlap below the molar ratio LMF/HSA, 1/1 and do not overlap above it. It seems that when there is less than 1 LMF molecule for 1 HSA molecule, only tryptophan residue takes part in the interaction, whereas above this number of LMF molecules, tryptophan and tyrosine residues participate in it. Moreover the quenching curves of HSA excited at 280 nm and in the presence of COL (Fig. 3b) are slightly higher than that excited at 295 nm. This means that, both tryptophan and tyrosine residues take part in the interaction. The synchronous fluorescence spectra were obtained by scanning simultaneously the excitation and emission monochromators. Thus, the synchronous fluorescence applied to the equation of synchronous luminescence [27]

$$F = kcdE_{ex}(\lambda_{em}-\Delta\lambda)E_{em}(\lambda_{em}) \quad (1)$$

where F is the relative intensity of synchronous fluorescence, $\Delta\lambda=\lambda_{em}-\lambda_{ex}$=constant, E_{ex} the excitation function at the given

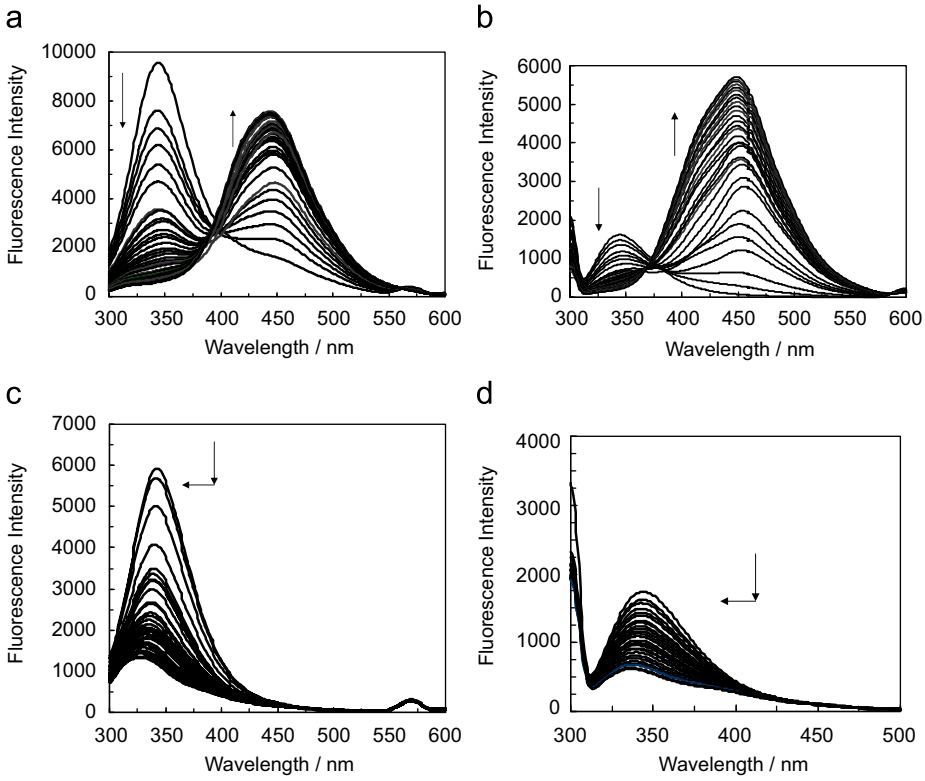

Fig. 2. Emission spectra of HSA in the presence of various concentrations of LMF (a), COL (b) at 298 K, pH=7.4 and λ_{ex}=280 nm. C (HSA)=1.5×10^{-6} mol L^{-1}; C (LMF)/($\times10^{-3}$ mol L^{-1}), C (COL)/($\times10^{-3}$ mol L^{-1}). The b and d parts correspond to the emission spectra of HSA in the presence of LMF and COL at λ_{ex}=295 nm. Arrows indicate the direction of the change. For the clarity of the spectra at the blue-shift, there are shown with arrows direction.

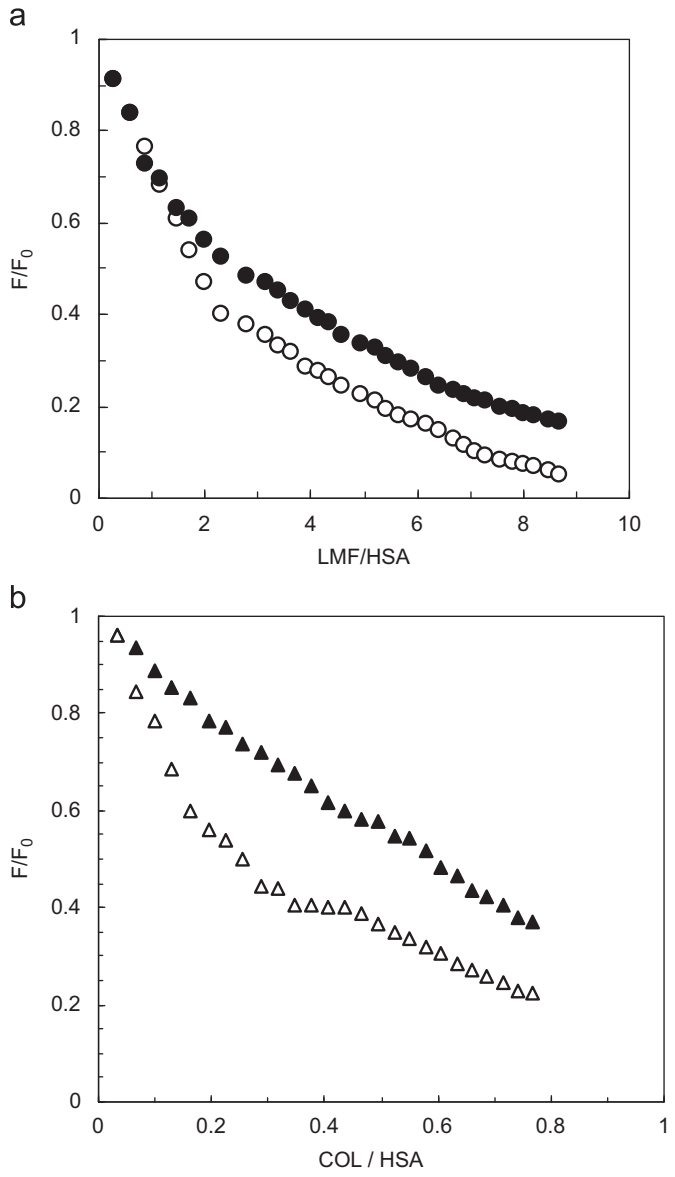

Fig. 3. Comparison of quenching curves of HSA excited at 280 and 295 nm in the presence of LMF (a) and COL (b). C (HSA)$=1.5\times10^{-6}$ mol L^{-1}; C (LMF)/($\times10^{-3}$ mol L^{-1}), C (COL)/($\times10^{-3}$ mol L^{-1}). Open symbols are at $\lambda_{ex}=280$ nm and filled symbols are at $\lambda_{ex}=295$ nm.

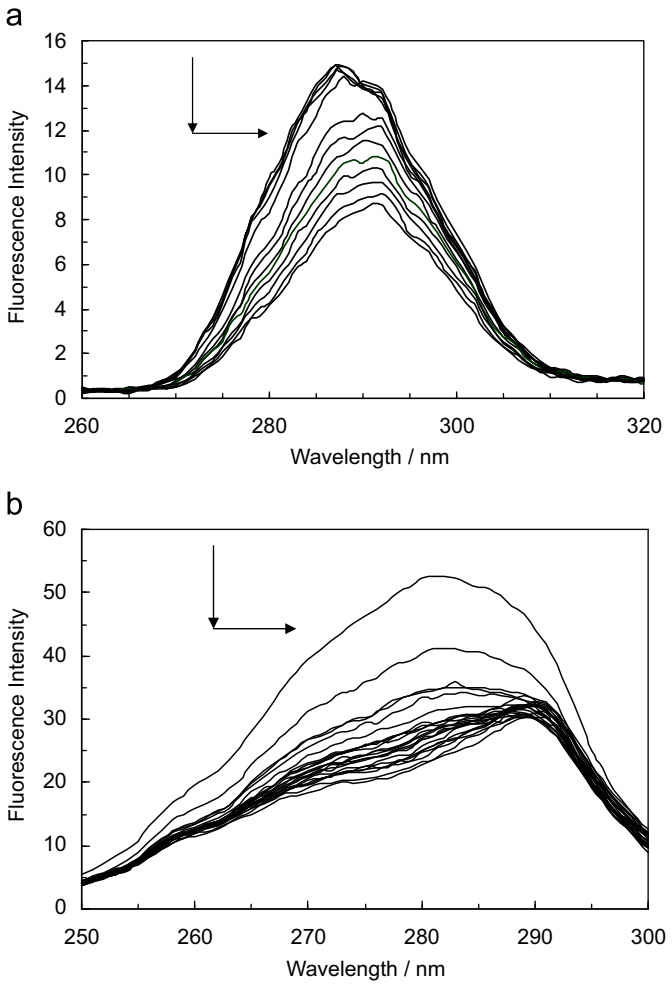

Fig. 4. Synchronous fluorescence spectrum of HSA: (a) $\Delta\lambda=15$ nm; (b) $\Delta\lambda=60$ nm; C (HSA)$=1.5\times10^{-6}$ mol L^{-1}; C (LMF)/($\times10^{-3}$ mol L^{-1}). Arrows indicate the direction of the change.

excitation wavelength, E_{em} the normal emission function at the corresponding emission wavelength, c the analytical concentration, d the thickness of the sample cell and k is the characteristic constant comprising of the "instrumental geometry factor" and related parameters. Since, the relationship of the synchronous fluorescence intensity (F) and the concentration of LMF and COL should follow the Eq. (1). F should be indirect proportion to the concentration of drugs. The optimal value of the wavelength intervals ($\Delta\lambda$) is important for the correct analysis and interpretation of the binding mechanism. When the wavelength interval ($\Delta\lambda$) was fixed at 60 nm of protein, the synchronous fluorescence has the same intensity as the emission fluorescence following excitation at 280 nm, just the emission maximum wavelength and shape of the peaks were changed [28–30]. Therefore the synchronous fluorescence measurements can deduce the binding mechanism as the emission fluorescence measurements did. Figs. 4 and 5 show the synchronous fluorescence at $\Delta\lambda=15$ and $\Delta\lambda=60$ of HSA in the absence and presence of LMF and COL, respectively. The synchronous fluorescence spectra of HSA with various concentrations of LMF at $\Delta\lambda=15$ nm (Fig. 4a) and $\Delta\lambda=60$ nm (Fig. 4b) show that the emission wavelength of the tyrosine and tryptophan residues are red shift with increase in concentration of LMF. It suggests that the tyrosine and tryptophan fluorescence spectrum may represent that the conformation of HSA is somewhat changed, leading to the hydrophilicity around tyrosine and tryptophan residues strengthened and the polarity increased [31]. Fig. 5 shows the effect of addition of COL on the synchronous fluorescence spectrum of HSA when $\Delta\lambda=15$ nm and $\Delta\lambda=60$ nm. The addition of the COL results in the fluorescence enhancement at both $\Delta\lambda=15$ nm and $\Delta\lambda=60$ nm. The emission wavelength of the tyrosine residues is red shift but no significant change in wavelength was observed in the tryptophan fluorescence emission. It means that the interaction of COL with HSA does not affect the conformation of tryptophan microenvironment. It is important to note that COL affect only the tyrosine residues present in HSA. This is because tyrosine contains one aromatic hydroxyl group unlike tryptophan. In addition, tyrosine can undergo an excited state ionization, resulting in the loss of the proton on the aromatic hydroxyl group. The hydroxyl group can dissociate during the lifetime of its excited state, hence the aromatic hydroxyl group present in the tyrosine residues is possible for the interaction of HSA with COL.

On the other hand, the Resonance Light Scattering (RLS) spectra of the system were recorded by synchronous scanning at $\lambda_{em}=\lambda_{ex}$ from 220–720 nm. The RLS spectra of the HSA-LMF and

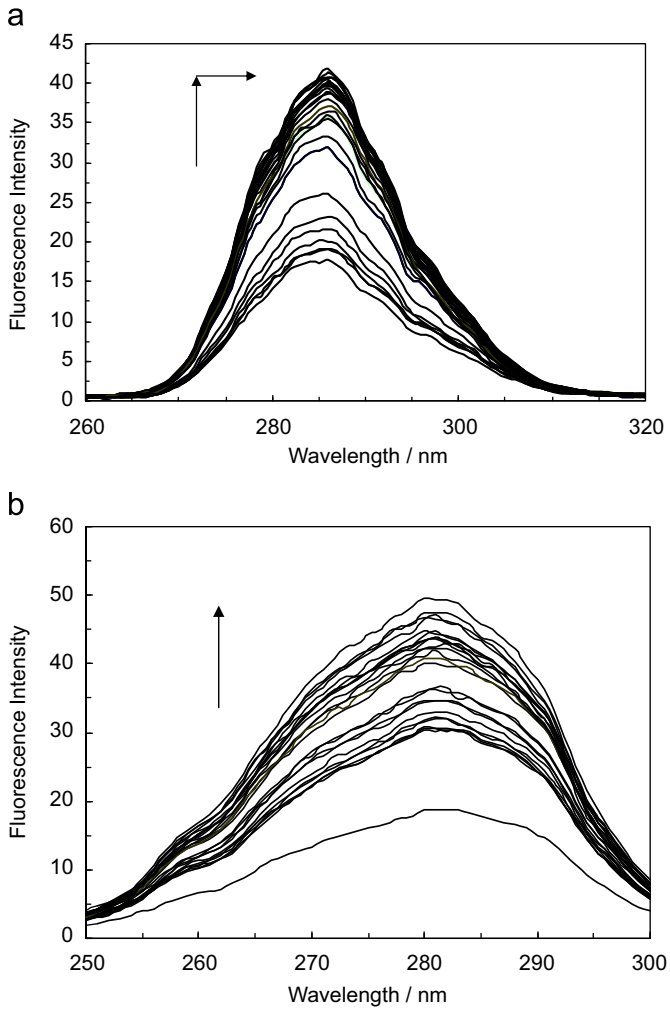

Fig. 5. Synchronize fluorescence spectrum of HSA: (a) $\Delta\lambda=15$ nm; (b) $\Delta\lambda=60$ nm; C (HSA)$=1.5\times10^{-6}$ mol L^{-1}; C (COL)/($\times10^{-3}$ mol L^{-1}). Arrows indicate the direction of the change.

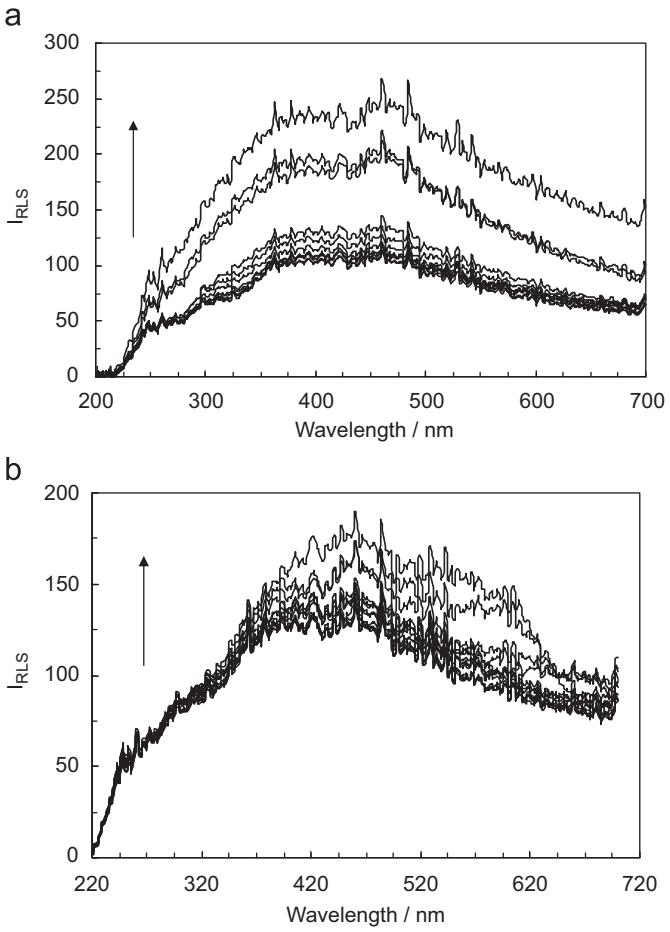

Fig. 6. Resonance light scattering spectra of HSA in the presence of different concentrations of LMF (a) and COL (b) at 298 K, pH=7.4. C (HSA)$=1.5\times10^{-6}$ mol L^{-1}; C (LMF)/($\times10^{-3}$ mol L^{-1}), C (COL)/($\times10^{-3}$ mol L^{-1}).

HSA-COL systems at physiological condition are shown in Fig. 6(a and b). The RLS intensity of the blank was very small and nearly constant. When LMF and COL drugs were added to HSA, the RLS intensity was greatly increased. It can be consequently concluded that LMF and COL interacted with HSA and produced a complex of which RLS intensity was much higher than that of HSA, LMF and COL when they existed separately.

3.2. HSA-LMF and HSA-COL interactions for the binary system

Generally speaking, the fluorescence quenching is the decrease in the quantum yield of fluorescence from a fluorophore induced by a variety of molecular interactions with quencher molecule, such as excited state reaction, molecules rearrangement, energy transfer, ground state complex formation and collision quenching. As the data shown in Fig. 2, the fluorescence intensity of HSA decreased regularly with the increasing concentration of LMF and COL. In order to confirm the quenching mechanism, the fluorescence quenching data are analyzed by the Lehrar equation [32]

$$F_0/\Delta F = 1/[Q]\times 1/f \times 1/K_Q + 1/f \quad (2)$$

where F_0 and ΔF are relative fluorescence intensity of protein in the absence and present of quencher [Q], respectively; ΔF, the difference between F_0 and F; f, the fractional accessible protein fluorescence; K_Q, the quencher constant; and [Q], the quencher concentration.

The original Stern–Volmer equation allows describing ligand movement within the fluorophore microenvironment when dynamic quenching occurs [33]

$$F_0/F = 1 + K_Q[Q] \quad (3)$$

where F and F_0 are fluorescence intensities of protein in the absence and presence of quencher [Q]; [Q], quencher concentration and K_Q the quenching constant.

Analysis of the Lehrer equation allowed us to determine the quenching constants K_Q and f values for HSA-LMF and HSA-COL (Fig. 7 (a and b)). The value of K_Q allows us to estimate the fluorophore availability for LMF and COL. The constant K_Q is a mean value of the quenching constants characterizing all binding sites of the HSA. Table 1 shows the K_{SV} and n for HSA-LMF and HSA-COL excited at 280 and 295 nm. The K_{SV} value of the quenching effect allows for the assessment of the affinity of LMF and COL to the HSA. The dependence of F_0/F on concentration of the drug allows us to determine the kind of quenching. If dependence forms a straight line then it points to dynamic quenching. A positive deviation points to both static and dynamic quenching. As can be shown from Figs. 7 and 8, dynamic quenching in the sub-domain where fluorophores occurs below the concentrations of LMF (0.0112 mM), COL (0.0108 mM) excited at 280 nm and LMF (0.0165 mM), COL (0.021 mM) excited at 295 nm for HSA-LMF and HSA-COL complexes, respectively. Above these concentrations, the positive deviation from the

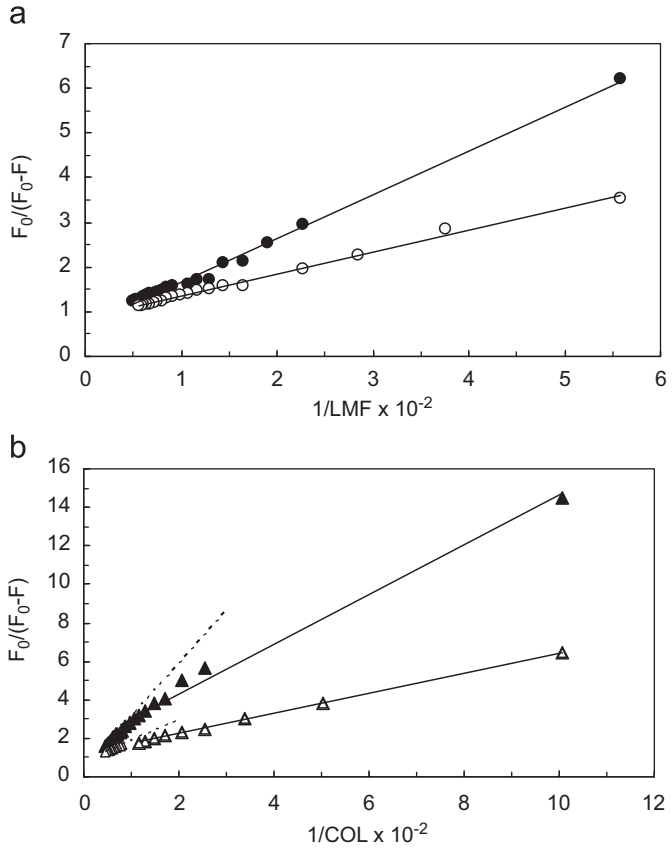

Fig. 7. The modified Stern–Volmer plots of the HSA-LMF (a) and HSA-COL (b) at pH=7.4. Open symbols are at λ_{ex}=280 nm and filled symbols are at λ_{ex}=295 nm.

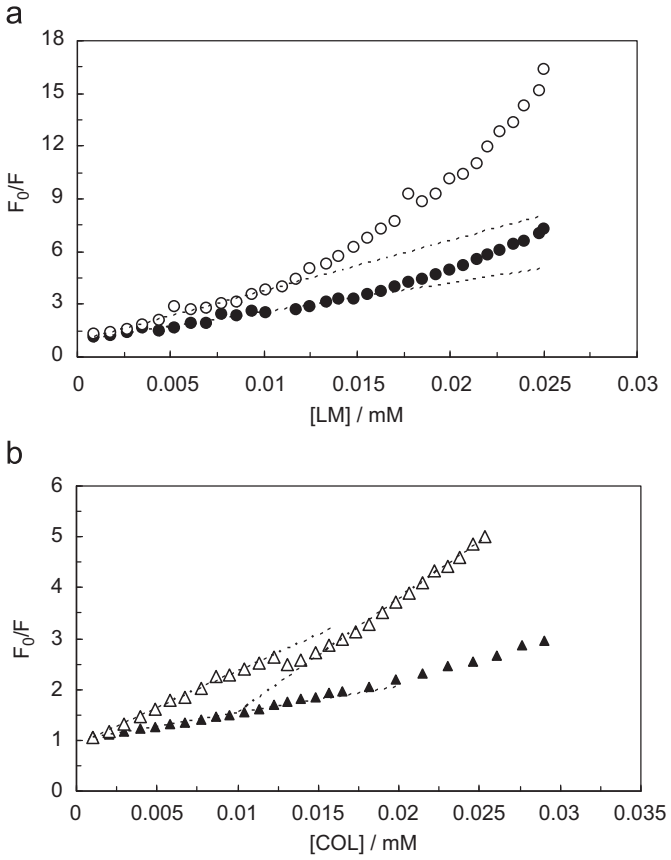

Fig. 8. The Stern–Volmer plots of the HSA-LMF (a) and HSA-COL (b) at pH=7.4. Open symbols are at λ_{ex}=280 nm and filled symbols are at λ_{ex}=295 nm.

straight line indicates that both the static and dynamic quenching is observed. A similar effect was observed for the ASA-SA system [34]. Table 1 shows that the values of quenching constants K_{SV} are higher for HSA-COL than for HSA-LMF system. This means that COL has a higher affinity to HSA than LMF. The highest values are determined at protein excitation of λ_{ex} 280 and 295 nm for all complexes.

Fluorescence quenching data of HSA were analyzed to obtain various binding parameters. The binding constant (K_a) and the number of binding sites (n) can be calculated according to the equation [35]

$$\log[(F_0-F)/F] = \log K_a + n\log[Q] \quad (4)$$

where F_0 and F are the fluorescence intensity without and with the drug, respectively. A plot of log $[(F_0-F)/F]$ vs. log $[Q]$ gave a straight line using least squares analysis whose slope was equal to n (binding sites) and the intercept on Y-axis to log K_a (K_a equal to the binding constant). Fig. 9 shows the plots of log $[(F_0-F)/F]$ vs. log $[Q]$ for the HSA-LMF and HSA-COL systems obtained from the flurometric titration. In Table 1, the binding constants and binding sites listed for HSA-LMF and HSA-COL binary systems. From Eq. (4), the values of K_a and n at 298 K were obtained to be 2.37×10^{-4} $Lmol^{-1}$ and 0.98 for HSA-LMF and 4.97×10^{-4} $Lmol^{-1}$ and 1.14 for HSA-COL, respectively, which implied that COL bounds strongly to HSA than LMF and there were one independent class of binding sites for both LMF and COL towards HSA. The linear coefficient R (0.9973 and 0.9987) indicated that the assumptions underlying the deviation of Eq. (4) were satisfactory [36].

To confirm how the protein structure is changed upon drug binding, changes in chirality are a good indication of ongoing folding changes and especially of tertiary and secondary structure modifications. Thus LMF, COL-induced conformational transitions of HSA were monitored by far UV-CD spectroscopy at different drug concentrations. The CD spectrum of HSA exhibits two negative bands about 208 and 222 nm (Fig. 10), which are characteristic of a high alpha-helical content. The values of the negative peaks at $[\theta]_{208}$ and $[\theta]_{222}$ for HSA-LMF slightly decrease which denotes that the secondary structure of HSA is not greatly affected by LMF (Fig. 10a). The molar ellipticity values of HSA-COL interactions show a more sever decrease, which arises from an unfolding process undergone by the protein in the presence of COL molecules. The results suggest that the conformational transition probably results in the exposure of the hydrophobic cavities and a perturbation of microenvironments around the deprotonated aromatic amino acid residues, which are favourable for the HSA adsorption onto the surface of COL.

3.3. HSA-LMF-COL and HSA-COL-LMF interactions for the ternary system

RLS spectra of HSA-LMF-COL and HSA-COL-LMF systems are shown in Fig. 11. It can be seen that, when COL and LMF were added, respectively, into the solution containing HSA-LMF and HSA-COL, the RLS intensity of the solution was enhanced. The most important experimental phenomenon is that RLS intensity of HSA-LMF and HSA-COL were enhanced in presence of COL and LMF, respectively. COL and LMF can interact with HSA-LMF and HSA-COL binary systems to form kinds of three-component complex (HSA-LMF-COL and HSA-COL-LMF) by hydrophobic and electrostatic interactions, which are the main reason of enhanced RLS intensity.

Table 1
Stern–Volmer quenching and binding constants of binary and ternary interaction of LMF and COL with HSA at pH=7.4.

System	$K_{SV} \times 10^4\ M^{-1}$ λ_{ex}=280 nm	$K_{SV} \times 10^4\ M^{-1}$ λ_{ex}=295 nm	R^a	$K_a \times 10^4\ M^{-1}$ λ_{ex}=280 nm	$K_a \times 10^4\ M^{-1}$ λ_{ex}=295 nm	n	R
HSA-LMF	2.86 ± 0.21	1.64 ± 0.22	0.9981	2.37 ± 0.19	1.55 ± 0.13	0.98	0.9973
HSA-COL	5.18 ± 0.17	1.44 ± 0.21	0.9975	4.97 ± 0.21	1.17 ± 0.24	1.14	0.9987
HSA-COL-LMF	0.413 ± 0.05	0.311 ± 0.05	0.9931	0.373 ± 0.04	0.293 ± 0.05	0.93	0.9954
HSA-LMF-COL	5.14 ± 0.19	1.36 ± 0.18	0.9976	4.88 ± 0.22	1.11 ± 0.08	1.09	0.9985

[a] R is the correlation coefficient.

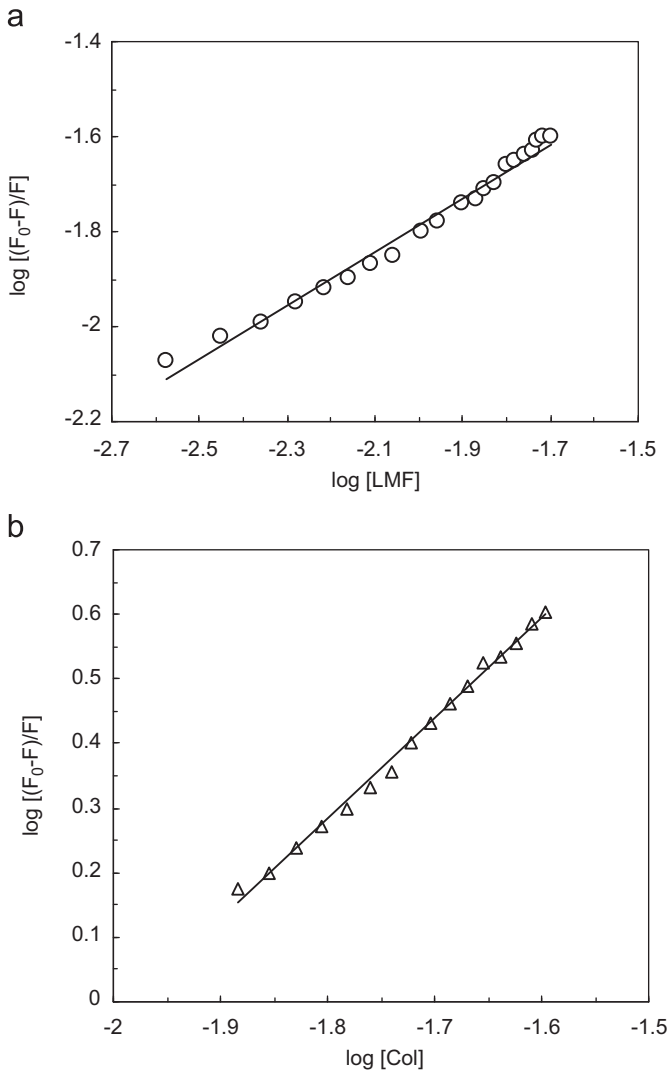

Fig. 9. Plots of log $[(F_0-F)/F]$ vs. log $[Q]$ at pH=7.4, λ_{ex}=280 nm, HSA-LMF (a) and HSA-COL (b).

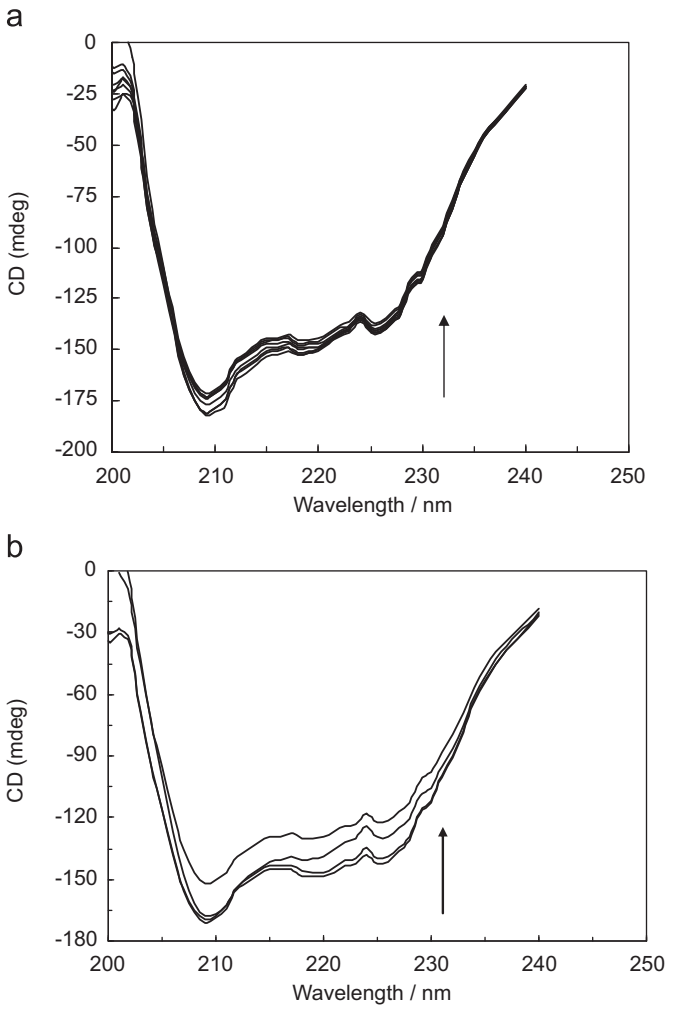

Fig. 10. Far UV-CD spectra of the HSA-LMF (a) and HSA-COL (b) systems. Arrows indicate the direction of the change.

Fig. 12 shows the quenching curves of ternary (HSA-LMF-COL and HSA-COL-LMF) systems in comparison with the binary systems at both 280 and 295 nm. The quenching curves of HSA-LMF and HSA excited at 280 nm in the presence of COL overlap. It means that only tryptophanyl residue participates in the both HSA-LMF-COL and HSA-COL interactions (Fig. 12a). This may suggest that COL does not affect or only weakly contribute to the quenching of HSA fluorescence in the presence of LMF in ternary system (HSA-LMF-COL). Fig. 12b shows the fluorescence quenching of HSA-COL in the presence of LMF at 280 and 295 nm do not overlap. It shows that in the interaction of LMF with HSA-COL, both tryptophanyl and tyrosyl groups take part. On the contrary, LMF influences the quenching of HSA by COL. In the presence of COL, the HSA fluorescence is significantly less quenched by LMF than when COL is absent. The presence of COL probably inhibits the formation of the HSA-LMF complex or makes the HSA-LMF interaction more difficult. COL reduces the affinity of LMF to HSA, displaces the LMF molecules and hinders the transfer energy due to the hydrophobic interactions stabilizing the complex. COL is bound to HSA with a low affinity. Therefore we should not exclude reciprocal interactions of both drugs within the sub-domain, which is common for this kind of binary of LMF and COL to HSA. This phenomenon can be caused by tyrosyl residues involved in forming the HSA-COL complex in sub-domain IIA

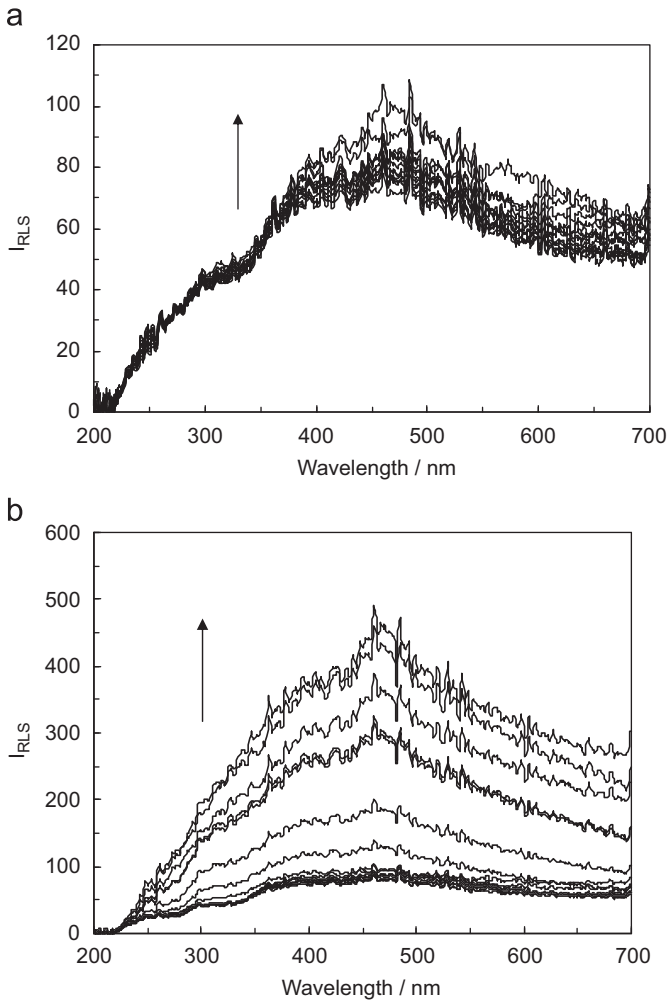

Fig. 11. (a) Resonance light scattering spectra of HSA-LMF in the presence of different concentrations of COL at pH 7.4 and 298 K. (b) Resonance light scattering spectra of HSA-COL in the presence of different concentrations of LMF at pH=7.4 and 298 K. C (HSA)=1.5×10^{-6} mol L^{-1}; C (LMF)/($\times10^{-3}$ mol L^{-1}), C (COL)/($\times10^{-3}$ mol L^{-1}).

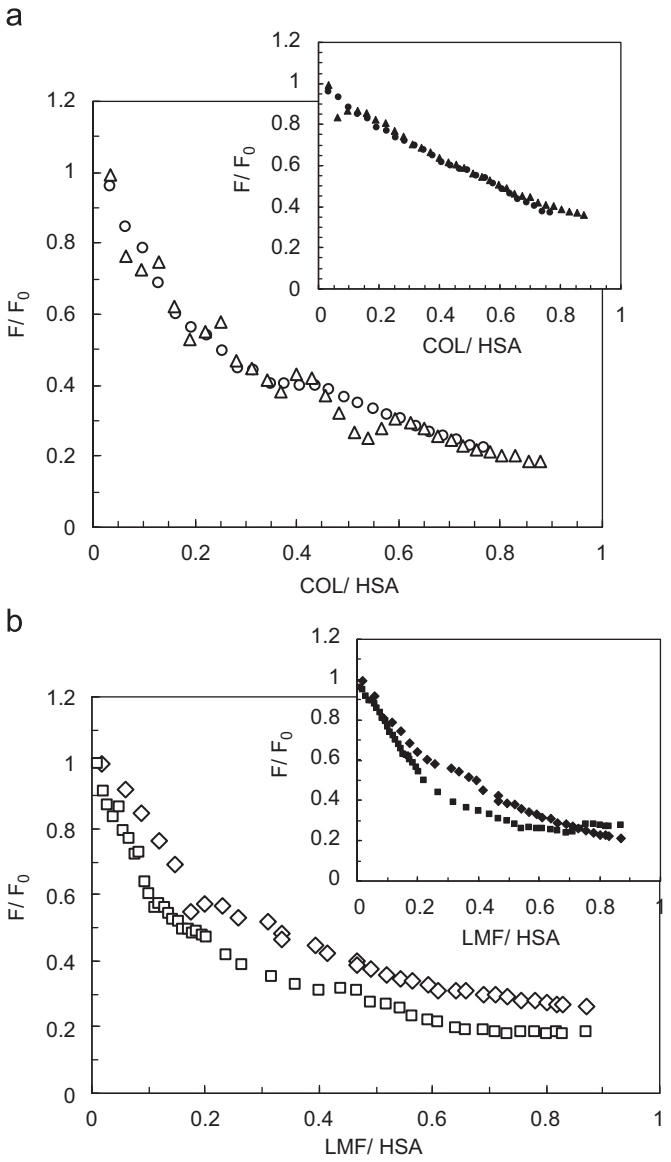

Fig. 12. (a) Comparison of quenching curves of HSA and HSA-LMF excited at 280 and 295 nm in the presence of various concentrations of COL. (b) Comparison of quenching curves of HSA and HSA-COL excited at 280 and 295 nm in the presence of various concentrations of LMF. Open symbols are at λ_{ex}=280 nm and filled symbols are at λ_{ex}=295 nm.

and/or IIIB/IIIA, where Tyrs are located. Fig. 12(b) confirms the Tyrs affect in the formation of HSA-LMF in the presence of COL. The fluorescence quenching of HSA-COL in the presence of LMF at 280 and 295 nm shows that both tryptophanyl and tyrosyl groups participate in the interaction between HSA-COL in the presence of LMF. The Stern–Volmer dependences of the ternary system for HSA excited at 280 and 295 nm is similar to binary system. Fig. 13 shows a positive derivation from the straight line for COL in the presence of LMF and for LMF in the presence of COL; indicate that both static and dynamic quenching is observed. Table 1 shows the quenching constants of binary and ternary systems determined on the basis of Stern–Volmer equation. It can be shown that Stern–Volmer constant for the ternary system HSA-LMF (constant)-COL is almost similar to the binary system of HSA-COL. It means that the presence of LMF in the system is not effective to the formation of HSA-COL complex. On the contrary, it can be observed from Table 1 that Stern–Volmer constant for the HSA-COL (constant)-LMF in a ternary system is lower than for the binary system of HSA-LMF. It can be concluded that the presence of COL in the system makes the formation of HSA-LMF complex difficult. These results indicate that a precaution is required in the treatment when the combination of LMF and COL is used at the same time, because each of them interferes with the binary of the other one to HSA. Table 1 shows the binding constants and binding sites for the ternary systems of HSA-LMF (constant)-COL and HSA-COL (constant)-LMF. The values of K_a and n at 298 K were obtained to be 4.88×10^{-4} $Lmol^{-1}$ and 1.09 for HSA-LMF (constant)-COL and 3.73×10^{-5} $Lmol^{-1}$ and 0.93 for HSA-COL (constant)-LMF, respectively, which implied that LMF dose not effect in the HSA-COL interaction, on the contrary, COL causes decrease in HSA-LMF interaction. The K_{SV} values in Table 1 confirm our results. To prove the possible influence of LMF and COL binding on the secondary structure of HSA-COL and HSA-LMF, the CD spectroscopy of ternary systems were measured. The fraction contents of different secondary structures for HSA-COL and HSA-LMF in the absence and presence of LMF and COL are shown in Table 2, respectively. A decrease in tendency of the alpha-helixes content and an increase in tendency of beta-sheet, turn and unordered structure contents were observed with the increase in concentration of LMF to the HSA-COL complex

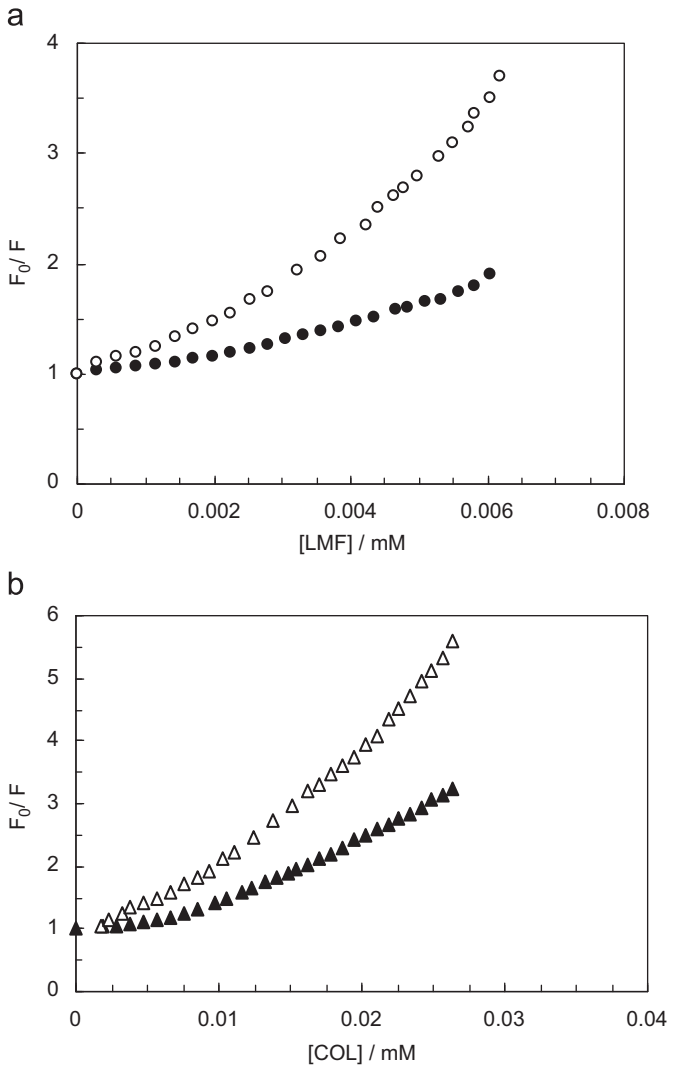

Fig. 13. (a) The Stern–Volmer plot of the HSA-COL in the presence of various concentrations of LMF at pH=7.4. (b) The Stern–Volmer plot of the HSA-LMF in the presence of various concentrations of COL at pH=7.4. Open symbols are at λ_{ex}=280 nm and filled symbols are at λ_{ex}=295 nm.

Table 2
Fractions of secondary structure of HSA in the absence and presence of LMF and COL in binary and ternary systems at pH=7.40.

System	f_α	f_β	f_t	f_u
HSA	53.94	18.33	13.54	14.19
HSA-LMF	50.43	19.53	14.34	15.70
HSA-COL	48.27	19.65	14.37	17.71
HSA-COL-LMF	48.03	19.11	14.51	18.35
HSA-LMF-COL	48.17	19.68	14.05	18.10

f_α, f_β, f_t and f_u are the fractions of alpha-helix, beta-sheet, turn and unordered coil.

(Table 2). As known, the secondary structure contents are related close to the biological activity of protein, thus a decrease in alpha-helical content from 50.43% to 48.03% meant the loss of the biological activity of HSA upon interaction with LMF in the presence of COL bound with the amino acid residues of the main polypeptide chain of protein and destroyed their hydrogen bonding networks [37], making the HSA adopt a more incompact conformation state and its exposure to the hydrophobic cavities.

Table 3
Docking of the COL and LMF into the whole rigid HSA.

	K_i	Binding energy	Intermolecular energy	Electrostatic energy
Colchicine in whole1H9Z	11.81 mM	−2.63	−3.91	−0.22
Lomefloxacin in whole 1H9Z	67.83 μM	−5.69	−6.49	−0.92

All these phenomena and analyses revealed that the binding of LMF and COL to HSA in the binary and ternary systems induced some conformational and micro-environmental changes in HSA.

3.4. Molecule modeling

Results of docking of the ligands into the whole protein (protein set to rigid) are shown in Table 3. COL shows less affinity to the protein than lomefloxacin. The determined high affinity area is shown in Fig. 14. Results of flexible dockings are shown in Table 4. It can again be implied from the results that binding affinity of LMF is far more than that of COL. It can also be concluded that previous attachment of COL reduces the affinity of LMF to HSA. However, the initial binding of LMF enhances the affinity of COL to the protein. COL or LMF when solely docked into the protein occupy the same pocket. COL forms a hydrogen bond with TYR161, for LMF though its orientation brings a nitrogen close to OH of the TYR161, it is a bit far away to form a stable hydrogen bond; however, it forms a hydrogen bond with LEU115 on the other end. COL's electrophile groups (oxygen containing groups) are surrounded by positively charged residues (ARG145, 196, 197, 117). Nitrogen of LMF's pyridine stands close to HIS146's aromatic group to form an electrostatic interaction. ARG186 is also close to the dihydroxyl portion of LMF though it is yet too far to form a hydrogen bond. LMF is also stabilized in the active site by formation of a hydrogen bond (Fig. 14a and b). In two-step dockings, the first ligand again fills the same pocket and the second ligand does not find the opportunity to get inside and binds superficially to the protein. COL when docked as secondary ligand is able to form a hydrogen bond with TYR138; however, there are no other noticeable interactions with the protein. This may describe lower affinity of COL as a secondary ligand (Fig. 14c). The story is different for LMF as a secondary ligand; it forms a good hydrogen bond with PHE134. The aromatic group of PHE134 stands to dihydroxyl portion of LMF. On the other end the NH of the pyrimidine group is close to the acidic side chain of GLU141, but there is a bit far to form a hydrogen bond

4. Conclusion

The quenching of relative fluorescence of human serum albumin proves to be an important tool for a better understanding regarding the crucial but specific changes occurring in the molecule. We studied the influence of an additional drug (LMF and COL) on changes in the affinity of HSA transport. On the basis of binding and quenching constants determined from Stern–Volmer equation it has been stated that an affinity to HSA is higher for COL than for LMF. The conclusions about the effect of one drug on the complex of the other with HSA have been presented by comparing the quenching of HSA fluorescence in the binary and ternary systems and by analyzing the binding constant values. It has been shown that COL induces the release or displacement of LMF from its binding sites in HSA molecule.

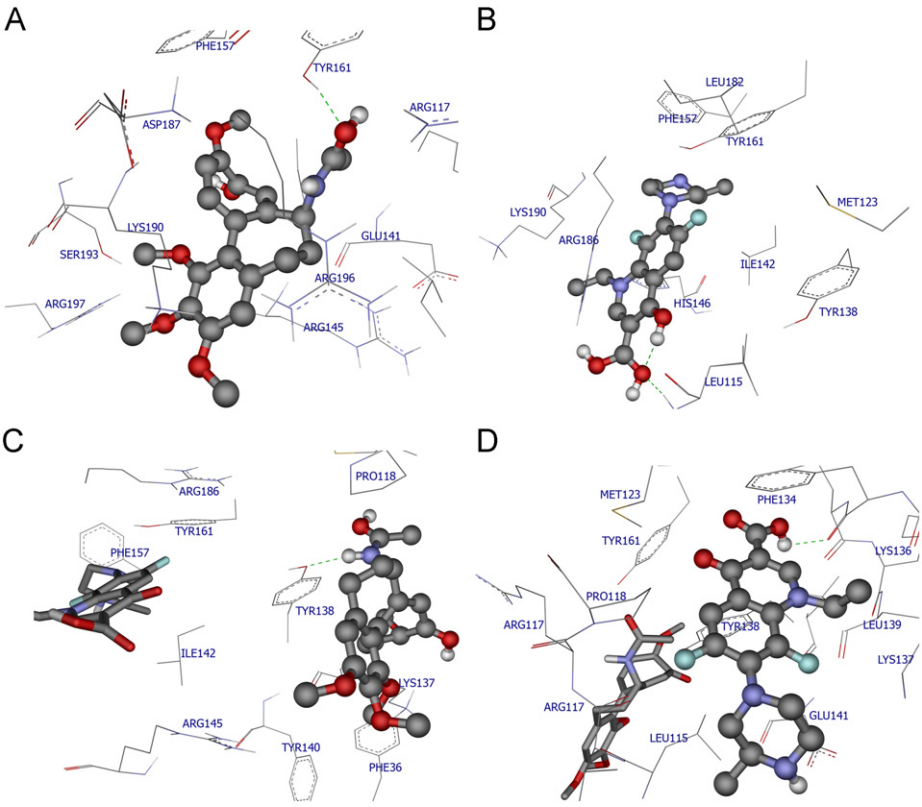

Fig. 14. Ternary interaction model between COL and HSA-LMF. (A,B) The binary interaction model between LMF and HSA. Only residues around 6.5 Å of LMF are displayed. The residues of HSA are represented using lines and the LMF structure is represented using a stick model. (C,D) The interaction model between COL and HSA-LMF. Protein atoms are shown in CPK representation and the LMF and COL structures are represented using a stick model.

Table 4
Flexible docking of the COL and LMF into the whole HSA.

	K_i	Binding energy	Intermolecular energy	Electrostatic energy
Colchicine in flexible active site	325.75 fM	−17.04	−5.1	−0.59
Lomefloxacin in flexible active site	809.14 aM	−20.59	−7.08	0.06
Colchicine into flexible active site with Lomefloxacin already docked	803.23 zM	−24.69	−6.42	−0.2
Lomefloxacin into flexible active site with Colchicine already docked	149.79 mM	−1.12	7.89	0.3

It probably inhibits the access of LMF to the HSA due to hydrogen bonding which may occur between COL and HSA. On the contrary, LMF dose not affect to the formation of the HSA-COL complex. The simultaneous presence of these drugs in binding to HSA indicates that precautions are required in the treatment when the combinations of these drugs used at the same time. This is due to the fact that each of them interferes with the binding of the other one to HSA.

Acknowledgements

The financial support of the Research Council of the Islamic Azad University-Mashhad Branch is gratefully acknowledged. The authors thank Dr. Ljungberg for English editing.

References

[1] D.C. Carter, J.X. Ho, Adv. Protein Chem. 45 (1994) 153.
[2] X.M. He, D.C. Carter, Nature 358 (1992) 209.
[3] T. Wang, B. Xiang, Y. Wang, C. Chen, Y. Dong, H. Fang, M. Wang, Colloids Surf. B: Biointerfaces 65 (2008) 113.
[4] M. Dockal, M. Chang, D.C. Carter, F. Ruker, Protein Sci. 9 (2000) 1455.
[5] T.J. Peters, in: All About Albumin. Biochemistry, Genetics and Medical Applications, Academic Press, Inc., New York, 1996.
[6] P.J. Sadler, J.H. Viles, Inorg. Chem. 35 (1996) 4490.
[7] I. Stanculescu, C. Mandravel, F. Delattre, D. Landy, P. Woisel, G. Surpateanu, J. Photochem. Photobiol. A: Chemistry 161 (2003) 79.
[8] U. Kragh-Hansen, Pharmacol. Rev. 33 (1981) 17.
[9] J. Tang, W. Wang, F. Luan, X. Chen, Int. J. Biol. Macromol. 37 (2005) 85.
[10] H.M. Zhang, Y.Q. Wang, M.L. Jiang, Dyes Pigm. 82 (2009) 156.
[11] W. He, Y. Li, J. Tian, H. Liu, Z. Hu, X. Chen, J. Photochem. Photobiol. A: Chem. 174 (2005) 53.
[12] U. Kragh-Hansen, V.T.G. Chuang, M. Otagiri, Biol. Pharma. Bull. 25 (2002) 695.
[13] J.H. Lin, D.M. Cocchetto, D.E. Duggan, Clin. Pharmacokinet. 12 (1987) 402.
[14] Y. Ni, X. Zhang, S. Kokot, Spectrochim. Acta Part A 71 (2009) 1865.
[15] X. Chen, J.C. Fan, Y. Wang, C.P. Fan, Z.C. Shang, Anal. Sci. 22 (2006) 427.
[16] R.G. Berger, J. Am. Acad. Orthop. Surg. 2 (1994) 255.
[17] J. Li, C. Ren, Y. Zhang, X. Liu, X. Yao, Z. Hu, J. Mol. Struct. 881 (2008) 90.
[18] A. Sulkowska, M. Maciazek-Jurczyk, B. Bojko, J. Rownicka, I. Zubic-Skupien, E. Temba, D. Pentak, W.W. Sulkowski, J. Mol. Struct. 881 (2008) 97.
[19] Y. Zhang, Y. Li, L. Dong, J. Li, W. He, X. Chen, Z. Hu, J. Mol. Struct. 875 (2008) 1.
[20] Y.Q. Wang, H.M. Zhang, G.C. Zhang, S.X. Liu, Int. J. Biol. Macromol. 41 (2007) 243.
[21] C.Z. Huang, Y.F. Li, X.D. Liu, Anal. Chim. Acta 375 (1998) 89.
[22] A.M. Khan, S. Muzammil, J. Musarrat, Int. J. Biol. Macromol. 30 (2002) 243.
[23] S. Era, K.B. Itoh, M. Sogami, K. Kuwata, T. Iwama, H. Yamada, H. Watari, Int. J. Pept. Protein Res. 35 (1990) 1.
[24] SYBYL Software, Version 6.9, Tripos Associates Inc., St. Louis, 2002.
[25] A. Pedretti, L. Villa, G. Vistoli, J. Mol. Graph. Model 21 (2002) 47.
[26] B. Valeur, in: Molecular Fluorescence: Principles and Applications, Wiley, VCH, Weinheim, 2002.
[27] S. Rubino, A. Gomez-Hens, M. Ualcarcel, Talanta 33 (1986) 633.
[28] J. Jin, X. Zhang, J. Lumin. 128 (2008) 81.
[29] J. Tang, F. Luan, X. Chen, Bioorg. Med. Chem. 14 (2006) 3210.
[30] J. Zhu, X. Zhang, D. Li, J. Jin, J. Mol. Struct. 843 (2007) 38.

[31] B. Klajnert, M. Bryszewska, Bioelectrochemistry 55 (2002) 33.
[32] S.S. Lehrer, Biochemistry 10 (1971) 3254.
[33] M.R. Eftink, C.A. Ghiron, Biochemistry 15 (1976) 672.
[34] B. Bojko, A. Sulkowska, M. Maciazek, J. Rownicka, F. Njau, W.W. Sulkowska, Int. J. Biol. Macromol. 42 (2008) 314.
[35] J. Kang, Y. Liu, M.X. Xie, S. Li, M. Jiang, Y.D. Wang, Biochim. Biophys. Acta 1674 (2004) 205.
[36] A. Sulkowska, M. Maciazek, J. Rownicka, B. Bojko, D. Pentak, W.W. Sulkowski, J. Mol. Struct. 834–836 (2007) 162.
[37] F.T. Cui, J. Fan, Z.D. Hu, Bioorg. Med. Chem. 12 (2004) 151.